Title Page

Task-related changes in aperiodic activity are related to visual working memory capacity independent of event-related potentials and alpha oscillations

Sian Virtue-Griffiths [a], Alex Fornito [a], Sarah Thompson [a], Mana Biabani [a], Jeggan Tiego [a], Tribikram Thapa [a], Nigel C Rogasch [a,b,c]

[a] Turner Institute of Brain and Mental Health, School of Psychological Sciences and Monash Biomedical Imaging, Monash University, VIC, Australia

[b] Discipline of Psychiatry, Adelaide Medical School, University of Adelaide, SA. Australia

[c] Hopwood Centre for Neurobiology, Lifelong Health Theme, South Australian Health and Medical Research Institute, SA, Australia

Correspondence

Sian Virtue-Griffiths

Email: sian.vitue-griffiths@monash.edu

Nigel C. Rogasch

Email: Nigel.rogasch@adelaide.edu.au

Address:

Monash University, Building 220, Clayton Campus,

770 Blackburn Rd. Clayton, VIC, 3800, Australia

Abstract

Individual differences in visual working memory capacity are related to slow-wave event-related potentials (ERPs) and suppression of alpha-band oscillatory power measured during the delay period of memory tasks using electroencephalography (EEG). However, recent evidence suggests that changes in the non-oscillatory, aperiodic features of the EEG signal may also contribute to working memory performance. We assessed several features of task-related changes in aperiodic activity including the spatial distribution, the effect of memory load, and the relationship between memory capacity, slow-wave ERPs, and alpha suppression. Eighty-four healthy individuals performed a continuous recall working memory task consisting of 2, 4 or 6 coloured squares while EEG was recorded. Aperiodic activity during a baseline and delay period was quantified by fitting a model to the background of the EEG power spectra using the FOOOF toolbox, which returned parameters describing the slope (exponent) and broadband offset of the spectra. The aperiodic exponent decreased (i.e., slope flattened) over lateral parieto-occipital electrodes but increased (i.e., slope steepened) over fronto-central electrodes during the delay period, whereas the offset decreased over parieto-occipital electrodes. These task-related changes in aperiodic activity were not altered by memory load. Larger increases in the aperiodic exponent were associated with higher working memory capacity measured from both the EEG task and a separate battery of complex span tasks, and this relationship was independent of slow-wave ERPs and alpha suppression. Our findings suggest that task-related changes in aperiodic activity during working memory are region specific and reflect an independent neural mechanism important for general working memory ability.

Keywords

Electroencephalography (EEG); Aperiodic activity; Working memory; Neural oscillations

Introduction

Working memory refers to the active maintenance of information in 'the mind' for brief periods to serve an ongoing task (Luck & Vogel, 2013). While working memory is domain general, there is also evidence for modality specific domains, often termed a phonological loop for verbal information and visuospatial sketchpad for visual information (Baddeley, 2012). The maximum amount of information that can be held at one time in visual working memory (VWM), known as working memory capacity, is limited between 1 to 5 items and varies between individuals (Logie, 2011). Differences in VWM capacity appear important for broader cognitive ability, accounting for approximately 45% of the variance in fluid intelligence (Fukuda et al., 2010). Furthermore, VWM capacity is reduced with healthy aging and in many neurological and psychiatric disorders (Berryman et al., 2013; Ding et al., 2015; Park & Gooding, 2014; Rock et al., 2014), with reductions often associated with functional outcomes such as poorer quality of life (Chehreh-Negar et al., 2012). Taken together, these findings suggest VWM is an essential cognitive ability for daily living.

Studies using electroencephalography (EEG) to record brain activity have identified several neural correlates of visual working memory capacity. For example, holding items in working memory is accompanied by a slow-wave event-related potential (ERP) during the delay period which is negative in polarity over posterior electrodes (Ruchkin et al., 1992; Ruchkin et al., 1995). This slow-wave ERP lateralises to the contralateral hemisphere when items are presented to a given visual field (often called contralateral delay activity) (McCollough, 2007; Vogel & Machizawa, 2004; Vogel et al., 2005), becomes more negative as memory load increases until an individual's capacity is exceeded (Vogel et al., 2004), and correlates with individual working memory capacity (Vogel & Machizawa, 2004, Vogel et al., 2005, Fukuda et al., 2015). Slow wave ERPs recorded during working memory tasks are also correlated with measures indexing attentional control, long-term memory, and fluid intelligence, indicating individual differences in delay activity are important for a broad range of cognitive abilities (Unsworth et al., 2015).

In addition to slow wave ERPs, working memory of visual items is accompanied by a suppression of oscillations in the alpha frequency range (8-12 Hz) during the encoding and delay period (Gevins et al., 1997; Sauseng et al., 2009). Like slow wave ERPs, alpha suppression lateralises to the contralateral

hemisphere when items are presented to a cued visual field, increases with memory load until an individual's capacity is exceeded, and correlates with working memory capacity, with greater suppression being associated with greater capacity (Fukuda et al., 2015). Increases in alpha-band oscillatory power are also observed over regions ipsilateral to relevant information in lateralized tasks, and later in the delay period in some working memory tasks, suggesting changes in alpha-band power may reflect a mechanism for gating information in working memory (Jensen & Mazaheri, 2010). The similarities between slow-wave ERPs and alpha suppression led to the proposal that these measures may reflect a shared neural mechanism (van Dijk et al., 2010). However, the slow wave ERP and alpha suppression account for independent variance in working memory capacity and occur across different time spans (Fukuda et al., 2015). Furthermore, recent studies using multivariate pattern analysis indicate that an item's spatial location can be decoded from alpha activity (Bae & Luck, 2018; Foster et al., 2016), whereas both spatial location and stimulus features (e.g., orientation) can be decoded from slow-wave ERPs (Bae & Luck, 2018), suggesting the two measures reflect independent neural mechanisms supporting working memory.

Although most EEG studies of working memory have focused on ERPs and/or oscillatory activity, neural signals also contain non-oscillatory, aperiodic activity. In the frequency domain, this aperiodic activity is represented by a 1/f-like distribution, with power decreasing exponentially as frequencies increase. Importantly, aperiodic activity can change over both short (e.g., during tasks (Podvalny et al., 2015)) and long (e.g., over the human lifespan (Voytek et al., 2015)) timescales, possibly reflecting changes in excitation/inhibition balance and other neural properties (Gao et al., 2017; Manning et al., 2009). Several methods have been proposed to separate aperiodic parameters from periodic oscillatory activity in neural power spectra. Using one approach, Voytek et al. (2015) showed the aperiodic exponent (representing the steepness of the 1/f-like slope in log-log space) was associated with age-related changes in working memory performance. In a more recent study, Donoghue et al. (2020) showed a decrease in both the aperiodic exponent (suggesting a flattening of the 1/f-like slope) and broadband offset (suggesting an overall reduction in broadband power) in posterior electrodes contralateral to attended items during the delay period of a working memory task compared to a baseline period. Importantly, the changes in aperiodic activity were independently associated with working memory performance from changes in alpha-band oscillatory

activity. Taken together, these studies suggest that changes in aperiodic activity may be important for working memory performance. However, most studies have focused on posterior electrodes, and it remains unclear how aperiodic activity changes across the scalp during working memory. Furthermore, it is unclear whether aperiodic activity is sensitive to changes in working memory load, and whether changes in aperiodic activity share a common neural mechanism with other EEG measures such as slow-wave ERPs.

The aim of this study was to comprehensively assess how aperiodic activity changes during a visual working memory task and how these changes relate to working memory performance. We assessed four main questions: 1) How does aperiodic activity change across the scalp during the delay period of a working memory task? 2) Are changes in aperiodic activity altered with increasing working memory load? 3) Are changes in aperiodic activity associated with working memory performance across individuals and tasks? and 4) Are changes in aperiodic activity independent from other EEG measures such as slow-wave ERPs and alpha suppression?

Methods

Participants

Eighty-four right-handed participants (28 males) aged 19-40 (M_{age} = 26.7, SD ± 4.9) were recruited for a multi-modal experiment including EEG, magnetic resonance imaging (MRI), transcranial magnetic stimulation (TMS), and cognitive testing. Only EEG and cognitive data were analysed in the current study. Exclusion criteria included: a history of neurological or psychiatric illness; colour-blindness; and contraindications to either MRI (Sawyer-Glover & Shellock, 2000), or TMS (Rossi et al., 2009). All participants had a predominantly Caucasian background (four grandparents of European descent) as the recruitment pool was also used for a separate genetics study. Experimental procedures were approved by the Monash University Human Research Ethics Committee (MURHEC number 8836).

Experimental design.

In the EEG session, participants were seated in a chair positioned approximately 480 mm from a computer monitor (monitor dimensions = 540 x 640 mm). Following preparation of the electrodes, EEG was recorded for an 8-minute "rest" period where participants sat quietly with their eyes open (data not analysed). Following the rest condition, participants performed a continuous recall working memory task. First, participants were provided with instructions on how to complete the task. Next, participants completed 2 control tasks testing motor precision (20 trials) and colour perception (30 trials) respectively, followed by a brief (~1 min) practice task. Participants then completed four blocks of the continuous recall task while EEG was recorded, taking 20-25 minutes to complete. In a separate cognitive assessment session held at least one day previous to the EEG session, participants completed a battery of computerised cognitive tasks including 3 complex span tasks which were also used to index working memory ability (see description below).

EEG acquisition

EEG was recorded from 62 passive electrodes in standard 10-10 positions (c-ring slit electrodes, EASCAP, Germany). The electrodes were referenced to FPz and grounded to AFz. The EEG signal was amplified (1000×), filtered (DC-2000 Hz), and digitised (10 kHz; Syamps2, Compumedics Ltd.) for offline analysis. Electrode impedance was reduced to <5 kΩ by applying abrasive gel with cotton tips and then conductive gel with blunt-ended syringes between the electrode and the skin. Electrode impedances were monitored regularly to ensure they remained minimal throughout the experiment.

Continuous recall working memory task

Participants performed a whole-field, partial report, continuous recall working memory task for colour (fig. 1; adapted from the MemToolbox; https://visionlab.github.io/MemToolbox/). Each trial began with a central fixation cross presented for 1500 ms (baseline period). Following the baseline period, a memory array of either 2, 4, or 6 coloured squares was presented for 500 ms (encoding period). The colours were randomly drawn from a continuous colour array (360 individual colours equally spaced across the colour spectrum; minimum difference of 24˚ between colours presented for each trial) and were presented in one of eight positions equally spaced around the fixation cross. Participants were instructed to remember as many squares as possible over the delay period, which consisted of a blank screen presented for 1000 ms. Following the delay period, greyed-out squares were presented in identical positions to the memory array with one target square highlighted by a black outline. Participants were asked to indicate the colour of the highlighted square from the memory array by moving a mouse cursor over a colour wheel with their right hand (note the orientation of the colour wheel was changed randomly between trials). The colour of the highlighted square updated instantaneously to match the position of the cursor on the colour wheel as the participant moved the cursor. Participants finalised their response by pressing the left mouse button and the baseline period for the next trial began. One hundred trials for each load were presented (total = 300 trials). Trials were presented in four blocks of 75 trials (25 trials of each load in a random order), with approximately 2-3 mins rest between each block.

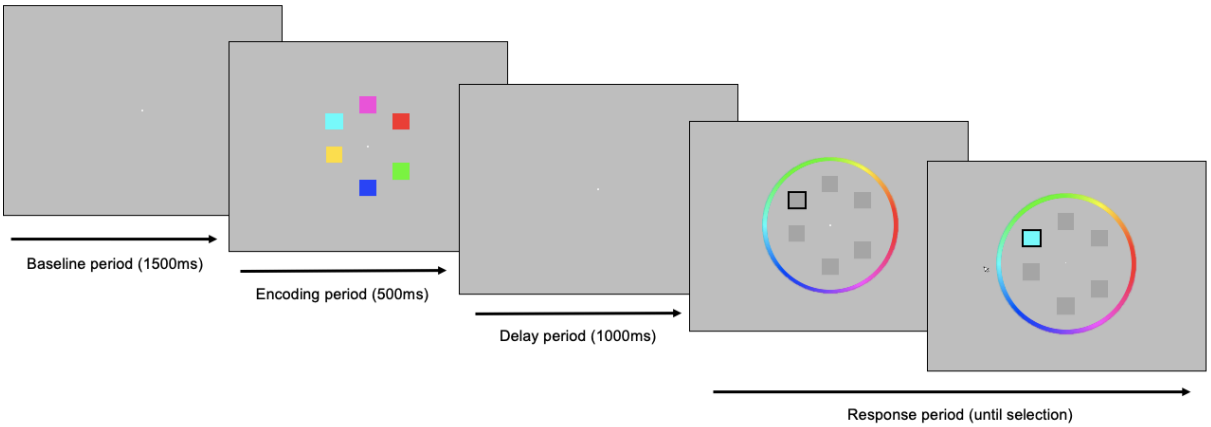

Figure 1. Continuous recall working memory task. Following a baseline period of 1500 ms, an array of either 2, 4 or 6 coloured squares was presented for 500 ms (encoding period). The squares were then removed for 1000 ms (delay period), after which a target square was indicated (black outline) and participants were instructed to match the colour as closely as possible on a colour wheel by navigating a mouse cursor (response period). The colour of the target square was instantaneously updated as the participant navigated around the colour wheel until the response was finalised by a button press.

Performance on each trial was quantified by calculating the distance between the target and the selected colour in degrees, resulting in a distribution of performance scores across trials for each load. Two measures of overall working memory ability (capacity and precision) were calculated for each load by fitting a standard mixture model (Zhang & Luck, 2008) to the performance distribution using a maximum likelihood approach implemented in the MemToolbox (Suchow et al., 2013). This approach returns two parameters optimized to the data: the guess rate, g, which reflects the probability the participant remembers nothing about the items and guesses randomly, and the standard deviation, σ, which is inversely proportional to the precision of the participants memory. Capacity (K) was calculated by multiplying the probability the participant had a representation of the item in memory (1- g) by the set size for each load (2, 4 or 6). Following the approach of Fukuda et al (2015), we also calculated the average K for

supracapacity set sizes (loads 4 and 6) to provide a single measure of visual working memory capacity for each individual (deemed *Kcd*).

EEG processing

EEG data were analysed using the EEGLAB (Delorme & Makeig, 2004), TESA (Rogasch et al., 2017), and FieldTrip (Oostenveld et al., 2011) toolboxes in MATLAB (R2015b, The Mathworks, USA) and the FOOOF toolbox (Donoghue et al., 2020) in Python (v3.6.5, Python Software Foundation). First, EEG data were downsampled to 1000 Hz. The data were then band-pass (0.1-100 Hz) and band-stop (48-52 Hz) filtered using the *eegfiltnew.m* function, epoched around the beginning of the encoding period (-1000 to 2000 ms; includes the baseline, encoding, delay, and first 500 ms of the response period), and baseline corrected (-500 to 0 ms). Data from the four separate working memory task blocks were then concatenated into a single file. Bad channels (electrodes with poor skin contact or that became disconnected) and bad trials (epochs contaminated by excessive muscle activity, large blinks/eye movements, motion artifacts etc.) were removed from the data following visual inspection (see supplementary table 1 for summary statistics). Residual artifacts were further minimised using independent component analysis (FastICA; Hyvärinen, 1999). Independent components were automatically categorised into neural and artifact components based on temporal, spatial and spectral characteristics using heuristic rules implemented in TESA. Categorisation was then visually assessed and components representing persistent muscle activity, eye blinks, lateral eye movements, or electrode noise were removed from the unmixing matrix before the data were reconstructed. Of note, persistent muscle activity can substantially alter the EEG power spectra and components representing muscle activity were selected using an approach validated using pharmacologic paralysis (Fitzgibbon et al., 2016). Missing electrodes were then replaced using spherical interpolation, and the data were re-referenced to the average of all electrodes. Remaining trials were then separated into each working memory load condition (2, 4 and 6).

Aperiodic activity and alpha-band oscillatory power

To characterise task-related changes in the EEG power spectra including aperiodic and oscillatory activity, EEG data from each epoch were converted into the frequency domain using Welch's method (*pwelch.m* function in MATLAB) across two time periods: a baseline period (-800 to 0 ms) and a delay period (650 to 1450 ms). The resulting power spectral density (PSD) estimates were then averaged over trials for each condition. To quantify aperiodic activity, the 1/f-like broadband background of the PSD from each time period and each electrode was fit between 3-30 Hz using the FOOOF toolbox. We limited the frequency range to <30 Hz to further minimise the contribution of any residual muscle activity on the spectra (Voytek et al., 2015). The methods used in the FOOOF toolbox are specifically designed to exclude oscillatory peaks from the fit, thereby ensuring an accurate estimate of aperiodic activity (Donoghue et al., 2020). The fitting approach returns two parameters: an exponent value which quantifies the steepness of the 1/f-like slope in log-log space; and an offset value which quantifies the broadband offset of the spectra. To quantify alpha-band oscillatory activity, mean power between 8-12 Hz was calculated from the PSD for each time period and each electrode. To ensure changes in alpha-band oscillatory power were not confounded by changes in aperiodic activity, the mean power was recalculated after subtracting the 1/f-like background from the PSD.

Slow wave ERPs

Slow wave ERPs were quantified by taking the mean EEG signal across trials for each electrode (i.e., the ERP) and then calculating the mean EEG voltage between 650 to 1450 ms, corresponding to the delay period.

Complex span working memory tasks

Three complex span working memory tasks (backward digit span, symmetry span, and operation span; fig. 2) were also administered in a separate session and used to determine whether relationships between EEG measures and working memory performance generalised beyond the continuous recall task

to broader measures of working memory ability. We used these tasks as capacity measures from complex span tasks and continuous recall/change detection tasks (also called visual array tasks) are thought to measure related components of working memory ability (Shipstead et al., 2015; Shipstead et al., 2012). Confirmatory factor analysis conducted in Mplus 8.3 (Muthén & Muthén, 1998) was used to quantify complex span performance, which extracts shared variance from related tasks, thus minimising the influence of task-specific components on performance estimates (Bollen, K. A., & Noble, 2011). To ensure adequate power to perform confirmatory factor analysis, we included data from an additional 34 participants who also completed the complex span tasks (total n = 118), resulting in an adequate case-to-parameter ratio of 39:1 (Jackson, 2003). Thus, complex span performance for a given individual represented a normalised value in relation to the overall sample included. Complex span tasks were completed using the Inquisit lab test library (Inquisit 5.011, 2016). Three tasks contributed to participants complex span factor score estimates: Backwards Digit Span (Woods et al., 2011), Operation Span (Unsworth et al., 2005) and Symmetry Span (Kane et al., 2004). Performance on each task was calculated by summing the load values of all accurately recalled trials. Factor score estimates were generated from the confirmatory factor analysis of the complex span factor using the regression method (DiStefano & Motl, 2009). Factor score determinacy was reasonably high (ρ = .816), indicating that the factor score estimates corresponded closely with the underlying latent variable (Grice, 2001).

Backwards Digit Span task. Participants were instructed to remember a sequence of single digit numbers, and then recall the numbers in reverse order by selecting them from a test screen (fig. 2A). Fourteen trials were conducted with between 2 to 8 numbers presented in each trial (i.e., 2 trials at each load).

Operation span task. Participants were required to remember the order of a series of alphabetical letter. Between letters, equations were presented and participants were required to judge whether the provided answer was true or false (fig. 2B). Following the final equation, participants were required to

recall the letters in correct order from a test screen. Fifteen trials were conducted with between 3 to 7 letters in each trial (i.e., 3 trials at each load).

Symmetry Span task. Participants were required to remember the order and location of a series of highlighted square on a 4x4 grid. Between each presented square, participants were required to judge whether another grid pattern was symmetrical or asymmetrical across the vertical axis (fig.2C). Following the final symmetry judgement, participants were required to indicate the location of the presented squared in order from a test screen. Twelve trials were conducted with between 2 to 5 squares presented in each trial (i.e., 3 trials at each load).

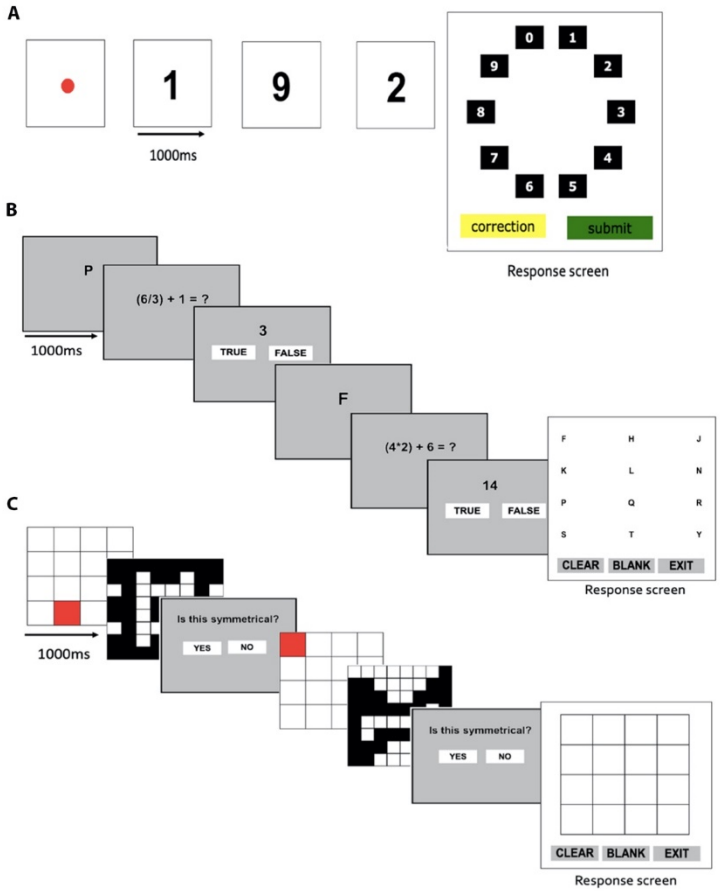

Figure 2. Complex span working memory tasks. Example trial of backwards digit span task (A), operation span task (B), and symmetry span task (C).

Statistics

To assess the effect of increasing memory load on working memory performance in the continuous recall task, a one-way repeated measures analysis of variance (ANOVA) was conducted on capacity and precision measurements (SPSSv24, IBM Corp, 2018). For EEG analysis, participants with more than 4 electrodes with a z-score >3 for a given measure of interest were removed to minimise the impact of extreme outliers on statistical analyses. Non-parametric, cluster-based permutation statistics were performed using Fieldtrip to determine the effect of task and load on aperiodic exponent, offset, alpha-band power and slow wave ERPs, (Oostenveld et al., 2011). Clusters were defined as two or more neighbouring electrodes in which the t-statistic exceeded a threshold of $p<0.05$ (two-sided dependent t-test). Monte Carlo p-values were calculated on 5000 random permutations and a value of $p<0.05$ (two-tailed unless indicated otherwise) was used as a cluster significance threshold for all analyses. To quantify effect sizes, mean Cohen's d values were calculated across all electrodes contributing to a significant cluster. To assess the relationship between EEG measures and working memory performance, we used the cluster-based permutation approach as outlined above, however electrode clusters were defined using a Spearman's correlation with a threshold of $p<0.05$. Finally, a multiple linear regression analysis was performed to assess whether aperiodic activity, alpha suppression and slow-wave ERPs were independently related to working memory performance. Input variables for each EEG measure were calculated using two different approaches: either by averaging across all electrodes contributing to significant clusters from the Spearman's correlation analysis, or by taking the individual electrode showing the strongest correlation.

Data and code availability

All data and code used in the analysis and to generate figures is available at: [available on publication].

Results

Performance on the continuous recall task

First, we assessed how increasing working memory load altered working memory performance. Shapiro Wilk statistic confirmed the assumption of normality was violated for load 2 (p=3.15x10^{8}), however, the sample size is robust to violations of normality (Tabachnick & Fidell, 2019). Greenhouse Geiser statistics were used due to violation of sphericity. Working memory capacity was altered with load (F=74.01, p=1.16 x 10^{-18}, η^2=0.47; ANOVA), with Bonferroni corrected post-hoc comparisons indicating that capacity increased from load 2 to load 4 (ΔM = -0.93, 95% CI =-1.07 -0.79, t(83) = -13.43, p=1.65 x 10^{-22}, d = 0.64) but not from load 4 to load 6 (ΔM = -0.19, 95% CI =-.39, -0.01, t(83) = -1.89, p=0.063, d = 0.21). Working memory precision was also altered with load (F=37.52, p<0.001, η^2= 0.31; ANOVA), with standard deviations increasing (i.e., precision decreasing) from load 2 to load 4 (ΔM = -8.33, 95% CI = -9.77, -6.88, t(83) = -11.46, p=8.79 x 10^{-19}, d = 6.66) and from load 4 to load 6, however this did not reach the threshold for significance (ΔM = -4.49, 95% CI = -8.23, -0.76, t(83) = -2.39, p=0.19, d = 17.21). Thus, our behavioural results are in line with other continuous recall and change detection tasks using coloured squares, showing a plateau in working memory capacity above 4 items (Luck & Vogel, 2013).

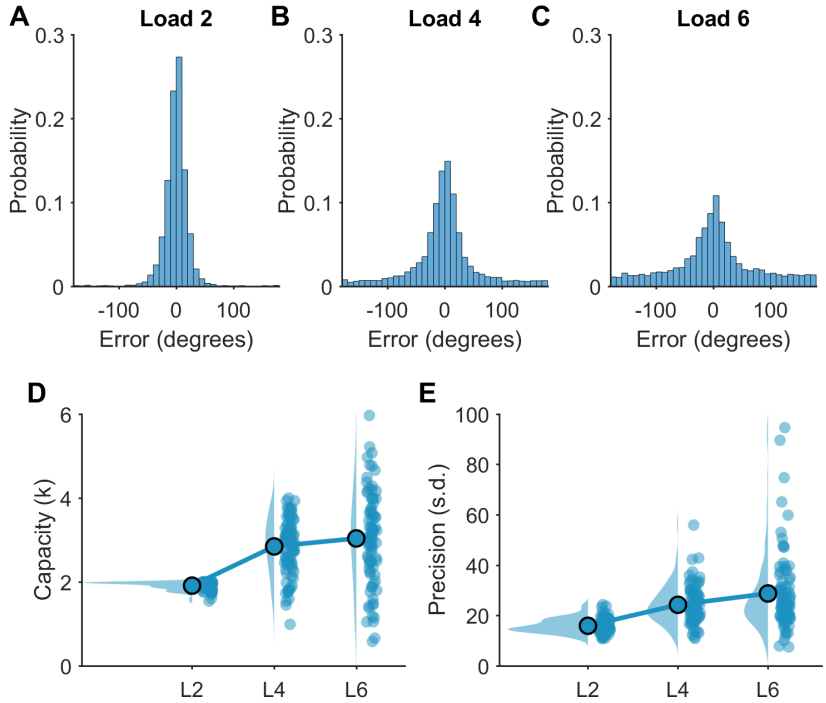

Figure 3. Working memory performance on the continuous recall task. A-C) Distribution of trial-by-trial performance calculated as error (distance from target in degrees) across all individuals (n=84) for each load. D-E) Working memory capacity (D) and precision (E) estimates at each load. Blue dots represent individual participants, highlighted blue dots indicate the group mean, and shaded blue area the distribution of the data.

Alpha-band oscillatory power and slow wave ERPs

Next, we attempted to replicate previously established EEG correlates of working memory capacity (Fukuda et al., 2015), including alpha-band oscillatory power and slow-wave ERPs. Alpha-band oscillatory power was reduced from the baseline to the delay period for each load (load 2, p =3.99 x10^{-4}, d = 0.52; load 4, p =3.99 x10^{-4}, d = 0.46; load 6, p =3.99 x10^{-4}, d = 0.52), and this suppression was stronger for load 4 compared to load 2 (p = 0.004, d = 0.29), but did not differ between load 4 and load 6 (no identified clusters; fig. 4). Removal of outliers altered the sample size of correlation between alpha suppression and WMC for the set size effect (n=80). The alpha suppression set-size effect had a negative association with working

memory capacity (p = 0.034, d = 0.28; 4E,G), indicating that stronger alpha suppression at supra-capacity loads was related to higher capacity. We could not find any associations between alpha suppression and complex span working memory capacity (n=79, no identified clusters, fig. 4F,H), suggesting alpha suppression was related to working memory components specific to the continuous recall task. Together, these findings replicated well-established capacity-limited effects on alpha suppression and relationships between alpha suppression and working memory capacity (Fukuda et al., 2015).

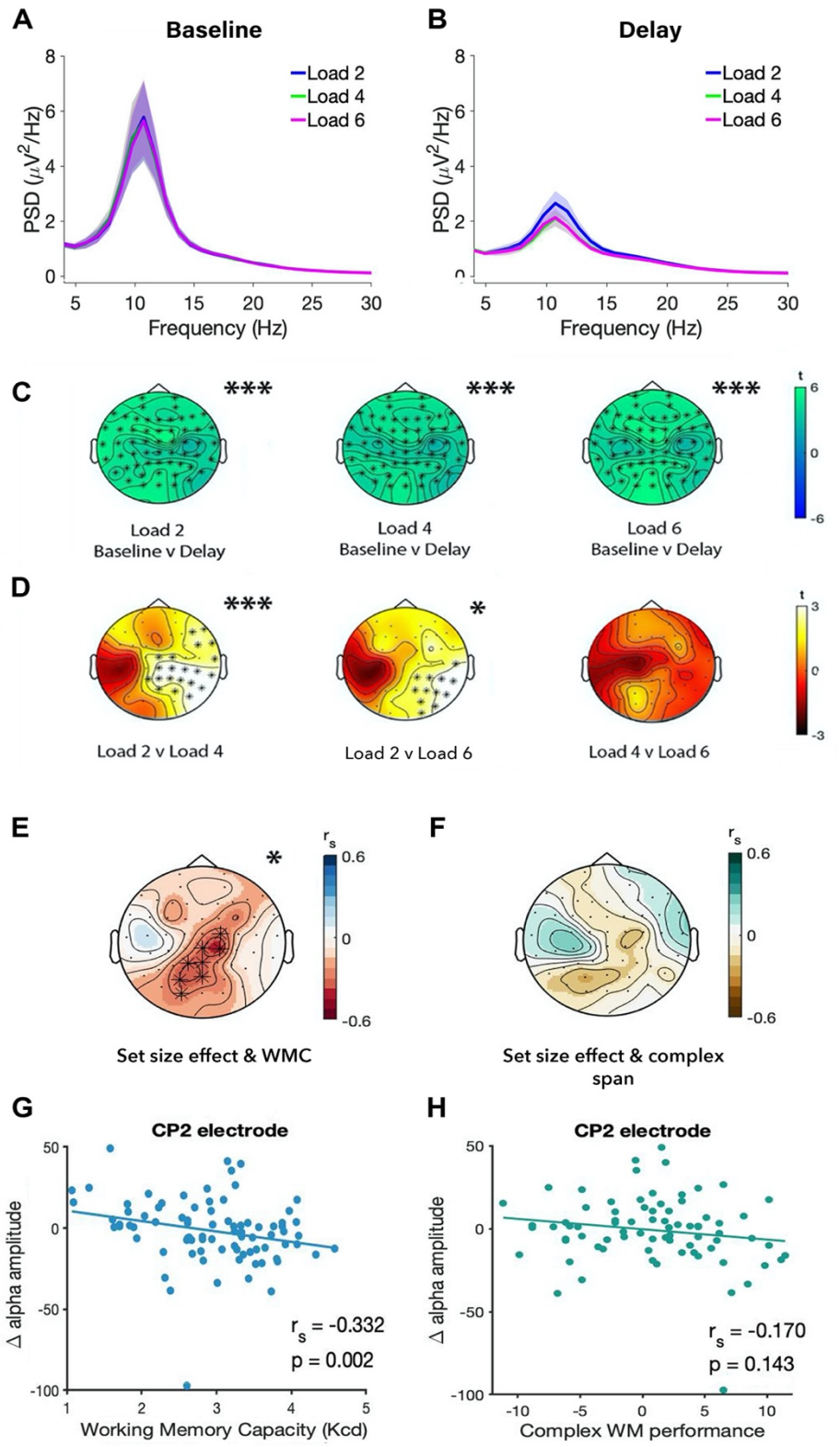

Figure 4. Changes in alpha-band oscillatory power with working memory. A-B) EEG power spectra (power spectral density, PSD) during the baseline (A) and delay (B) period for each load. Solid line represents the group mean and shaded bars the standard error. C) Topoplots indicating changes (t-statistics)

in alpha-band oscillatory power between the baseline and delay periods across all electrodes. D) Topoplots indicating differences (t-statistics) in task-related alpha suppression between loads across all electrodes. E-H) Topoplots demonstrating the relationship (Spearman's rho, r_s) between task-related changes in alpha-oscillatory power and working memory capacity (E) and complex span performance (G) at each electrode (left column), and scatter plots for a centroparietal electrode (CP2, right column; F and H). Data are plotted for the set size effect. * indicate electrodes contributing to significant clusters ($p<0.05$).

Slow wave ERPs during the delay period changed in amplitude between load 2 to load 4 increasing over frontal electrodes, ($p = 0.032$ $d = 0.34$), and decreasing over parietal electrodes ($p = 3.999 \times 10^{-4}$, $d = 0.39$, fig. 5C). However, there was no significant difference in the slow wave ERP between load 4 to load 6 ($p = 0.222$), indicating a plateau in amplitude increases at supra-capacity loads. Removal of outliers altered the sample size of correlations between the slow wave ERP and working memory at load 4 (n=79), load 6 (n=76) and the set size effect (n=79).The slow wave ERP set-size effect did not show a significant relationship with working memory capacity at the cluster level ($p = 0.240$), although qualitatively a greater reduction in ERP amplitude was negatively associated with higher working memory capacity in some frontal electrodes (p=0.039, $d = 0.28$, one tailed; fig. 5E-F). Furthermore, the slow wave ERP set size effect (n=77) was associated with complex span performance ($p = 0.010$, $d = 0.30$) with a negative relationship over frontal electrodes and a positive relationship over occipital electrodes (fig. 5G-H). Together, these findings replicate established capacity-limited load effects on slow wave ERP amplitudes and relationships between changes in slow-wave ERPs with loads and broader measures of working memory capacity (Fukuda et al., 2015; Unsworth et al., 2015).

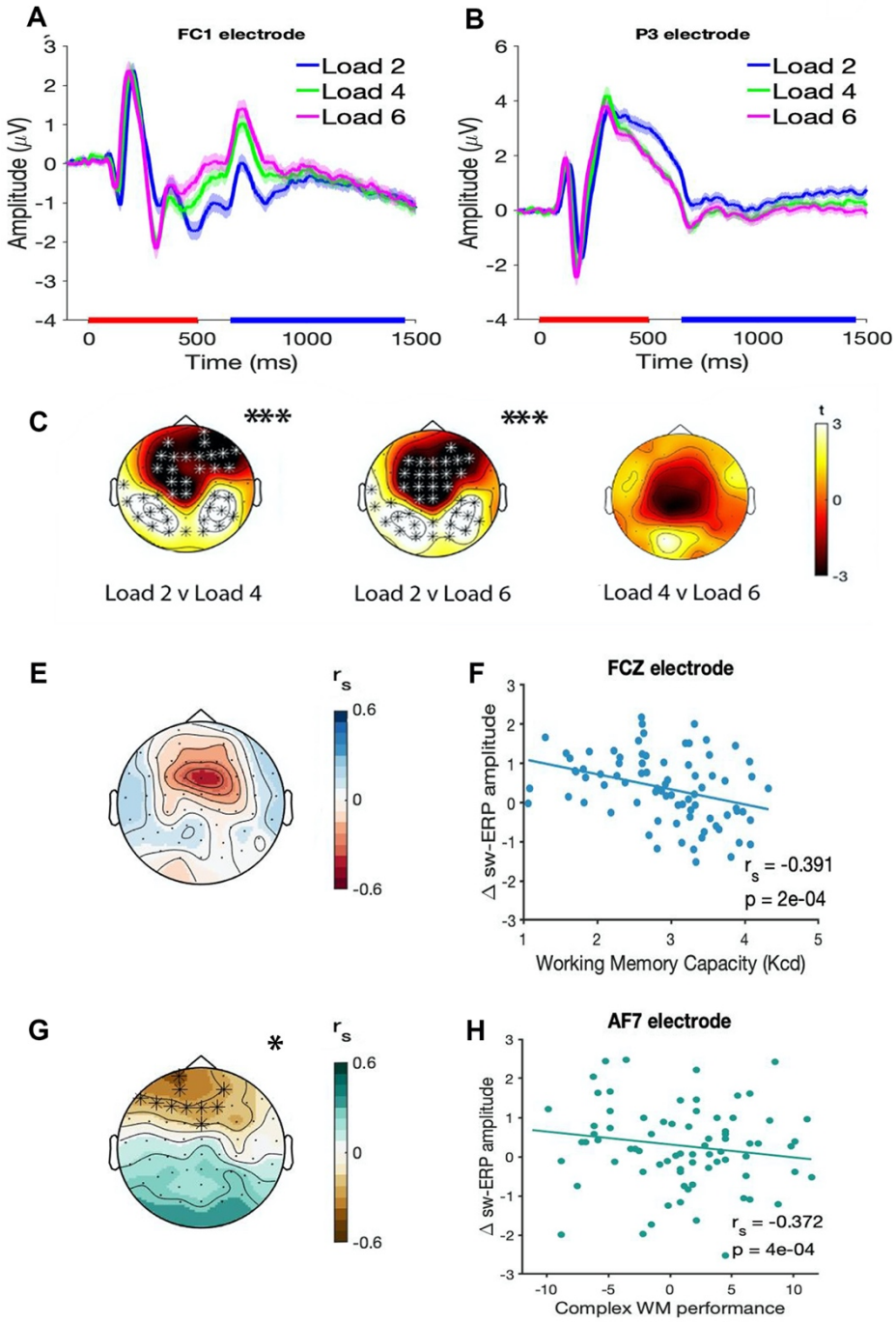

Figure 5. Changes in slow-wave event-related potentials (ERPs) with working memory. A-B) ERPs from a left frontal (FC1, A) and parietal (P3, B) electrode at different working memory loads. The red bar on the x-axis represents the timing of the stimulus (0-500 ms), with the slow-wave ERP period being analysed from 650-1450 ms (blue bar on the x-axis). C) Topoplots indicating differences in slow-wave ERP amplitude during the delay period between loads across all electrodes. E-H) Topoplots demonstrating the

relationship (Spearman's rho, rs) between slow-wave ERP amplitude changes with load and working memory capacity (E) and complex span performance (G) at each electrode (left column), and scatter plots for a frontocentral electrode (FCZ, F) and left fronal electrode (AF7, H) respectively. Data are plotted for the set-size effect. * indicate electrodes contributing to significant clusters (p<0.01).

Effect of task on aperiodic activity

Next, we assessed whether aperiodic activity changed during different periods of the working memory task. The aperiodic exponent differed from the baseline to the delay period in load 2 (p = 3.99 x10^{-4}, d = 0.33), load 4 (p = 3.99 x10^{-4}, d = 0.36) and load 6 (p = 1.99 x10^{-4}, d = 0.30, p = 0.006, d = 0.38), with exponent values increasing (i.e., slope steepening) in frontocentral electrodes, but decreasing (i.e., slope flattening) in lateral occipitoparietal electrodes (fig. 6). The aperiodic offset also changed over the task in load 2 (p =3.99 x10^{-4}, d = 0.42), load 4 (p =3.99 x10^{-4}, d = 0.36), and load 6 (p =3.99 x10^{-4}, d =0.39), decreasing during the delay period in occipitoparietal electrodes (fig. 6). Thus, both the aperiodic exponent and offset were altered during the delay period of working memory, however the direction of this change differed across the scalp.

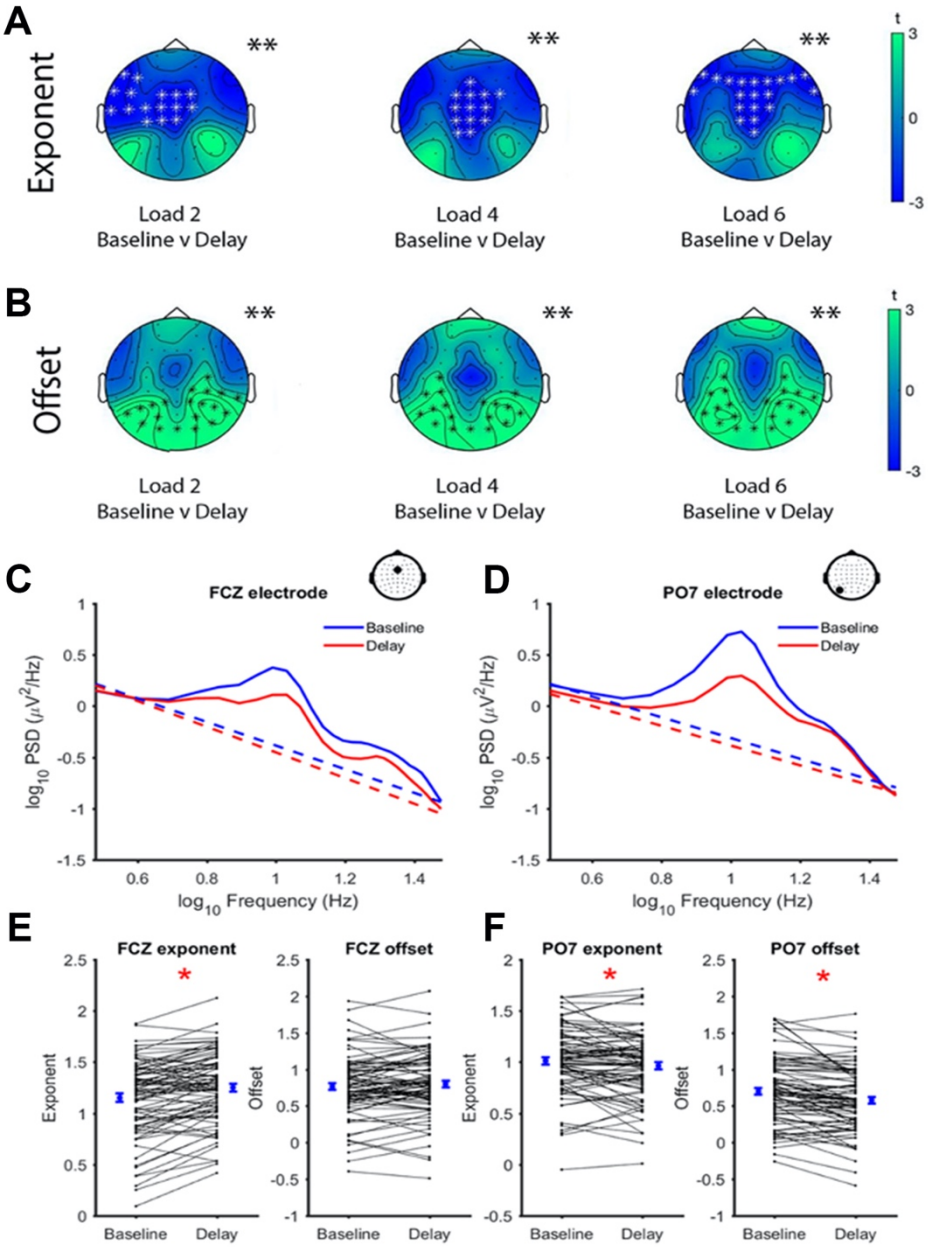

Figure 6. Task-related changes in aperiodic activity across the scalp. Topoplots representing changes (t-statistics) in aperiodic exponent (A) and offset (B) values between the baseline and delay periods of the working memory task at each load. * indicate electrodes contributing to significant clusters (p<0.01). C-D) Group mean EEG power spectra (solid lines) and aperiodic activity (dashed lines) from a frontocentral (C; FCZ) and lateral occipitoparietal (D; PO7) electrode during the baseline (blue) and delay (red) period of load 4. Data are plotted in log-log space. Inset topoplots indicate the position of the electrode on the scalp. E-F) Group mean (blue dots; ± standard error) and individual (black dots and lines) changes in aperiodic

exponent and offset values from baseline to delay for frontocentral (E; FCZ) and lateral occipitoparietal (F; PO7) electrodes. * indicate a significant difference between time periods (p<0.05; paired t-test).

Effect of working memory load on aperiodic activity

Having established that aperiodic activity is altered during the delay period of working memory, we next asked whether the magnitude of these changes differed with increasing memory load. We could find no evidence for meaningful differences in task-related changes in aperiodic exponent or offset values when comparing memory loads (*no identified clusters*; fig. 7). These findings indicate that while the properties of aperiodic activity changed during the delay period, these task-related changes were of a comparable magnitude regardless of the memory load.

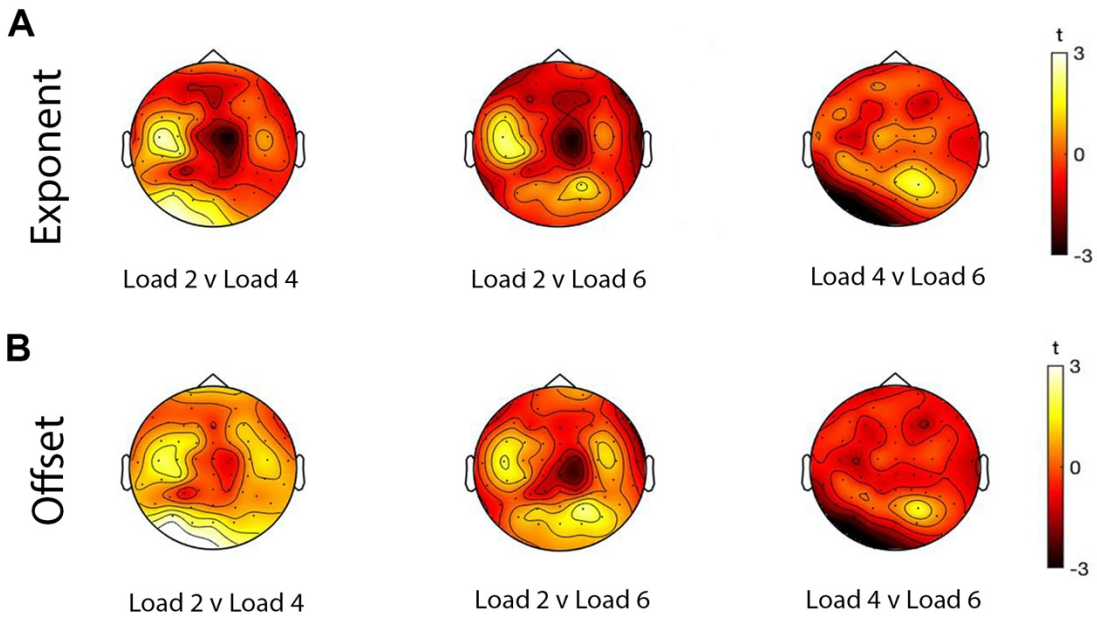

Figure 7. Load-dependent changes in task-related aperiodic activity. Topoplots representing differences (t-statistics) in task-related changes in aperiodic exponent (A) and offset (B) values between different memory loads. There were no significant clusters for any comparison (all p>0.05).

Relationship between changes in aperiodic activity and working memory performance

Next, we asked whether task-related changes in aperiodic activity were related to working memory performance across individuals. Removal of outliers altered the sample size of analyses for the aperiodic exponent at load 4 (n=82), load 6 (n=81), and the set size effect (n=82) and for the offset at load 4 (n=83) and load 6 (n=81). Task-related changes in aperiodic exponent values were positively associated with working memory capacity (quantified as *Kcd*; the mean capacity for suprathreshold loads 4 and 6; see Fukuda et al, 2015) at load 6 (p = 0.006, d =.30) and load 4 (p = 0.048, d =.30), however this did not reach the threshold for significance at load 4 and there were no clusters identified at load 2 (fig. 8A-F). Although we didn't observe any load-dependent changes in aperiodic activity (fig. 7), we also assessed whether set-size effects (the mean change in aperiodic slope for supra-capacity loads 4 and 6 subtracted from sub-capacity load 2) were related to working memory capacity, as these relationships have been reported for other EEG measures (Fukuda et al., 2015). Aperiodic exponent set size effects were also positively correlated with working memory capacity (p = 0.041, d =.30; fig. 8G-H), however this did not reach the threshold for significance when accounting for multiple comparisons. In contrast, we could not find evidence for meaningful associations between aperiodic offset and capacity at any load, or between any of the parameters and working memory precision (load 2, *no clusters*; load 4, p= 0.106; load 6, p= 0.074, set-size effect, *no clusters*). These findings indicate that individuals who showed larger increases in aperiodic exponent (i.e., steeper slopes) in frontocentral electrodes during the delay period at supra-capacity loads have higher working memory capacity.

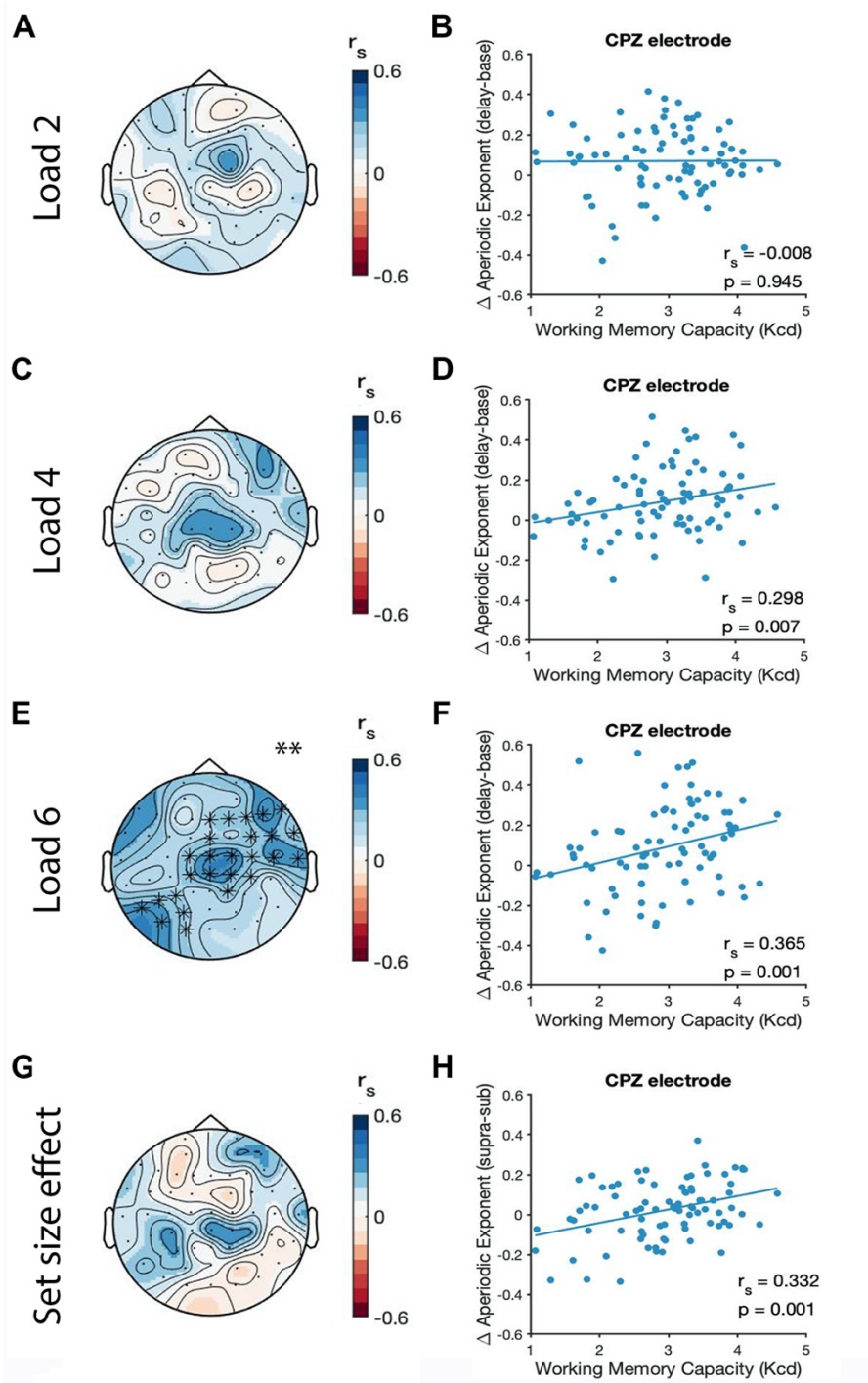

Figure 8. Relationship between task-related changes in aperiodic exponent and working memory capacity. Topoplots demonstrating the relationship (Spearman's rho, r_s) between task-related changes in the aperiodic exponent and working memory capacity at each electrode (left column), and scatter plots for a centroparietal electrode (CPZ, right column). Data are plotted for each load and the set size effect. ** indicate electrodes contributing to significant clusters (p<0.01).

We then asked whether the relationship between changes in aperiodic activity and capacity generalised to measures of working memory ability from complex span tasks. Factor score estimates of complex span performance were related to working memory capacity (Kcd) from the continuous recall task (p = 0.017; Pearson's correlation). Additionally, estimates of complex span performance were also positively associated with task-related changes in aperiodic exponent at load 4 (p = 0.045; one-tailed) and load 6 (p = 0.039; one-tailed), although these did not reach the threshold for significance and no clusters were identified for the set size effect (fig. 9). Together, these findings suggest that task-related changes in aperiodic activity index a neural mechanism which is important for general working memory ability, as opposed to task-specific effects.

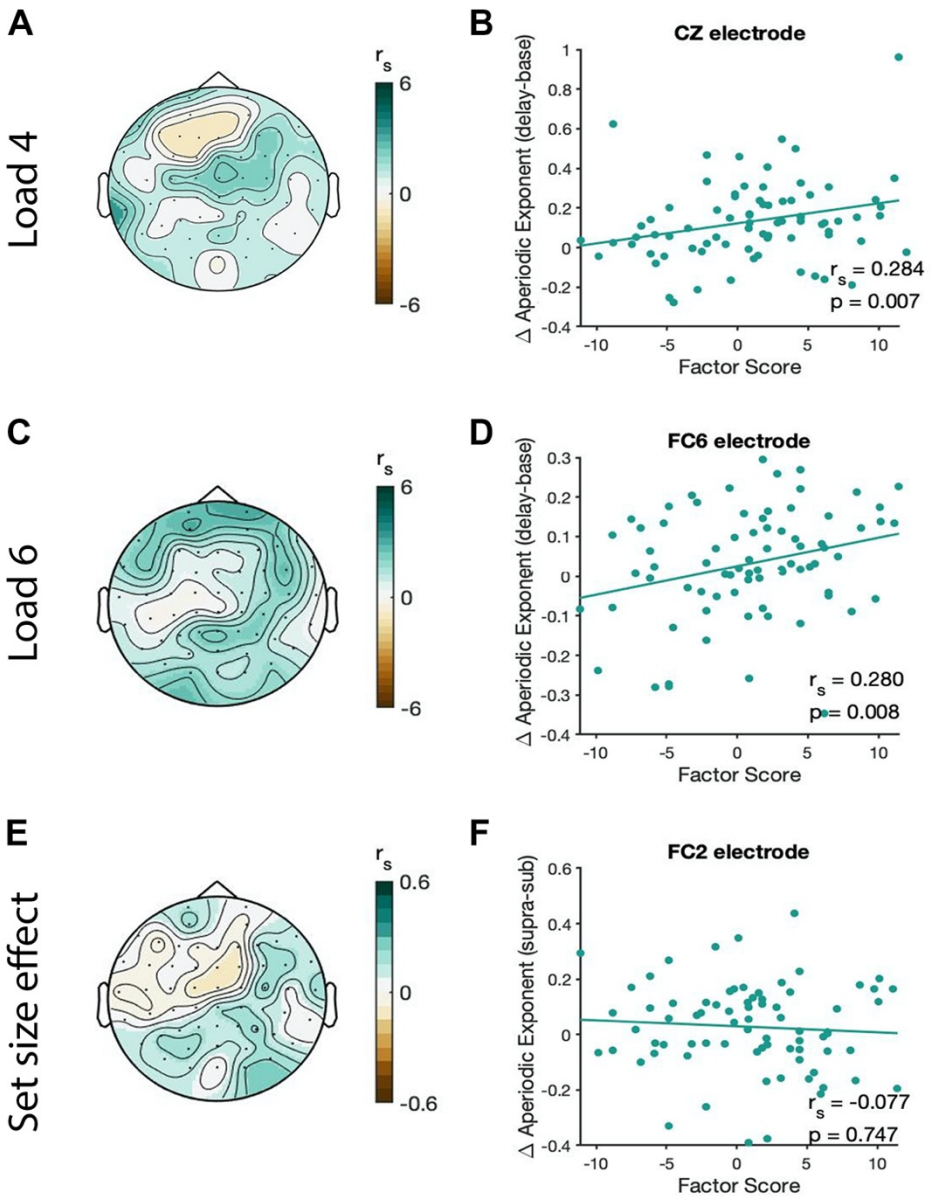

Figure 9. Relationship between task-related changes in the aperiodic exponent and complex span working memory capacity. Topoplots demonstrating the relationship (Spearman's rho, r_s) between task-related changes in the aperiodic exponent and complex span working memory capacity (represented as a factor score) at each electrode (left column), and scatter plots from electrodes showing peak correlations (right column). Data are plotted for loads 4, 6 and the set size effect.

Aperiodic corrected alpha suppression

Having characterised the aperiodic activity from the power spectra, we then set out to determine whether accounting for aperiodic activity changed alpha suppression during VWM by subtracting the 1/f-like background from the power spectra. Again, corrected alpha-band oscillatory power was reduced from the baseline to the delay period for each load (load 2, p =3.99 x10^{-4}, d = 0.51; load 4, p =3.99 x10^{-4}, d = 0.45; load 6, p =3.99 x10^{-4}, d = 0.51), and this suppression was stronger for load 4 compared to load 2 (p =0.006, d = 0.29), and load 6 compared to load 2 (p =0.032, d = 0.28), but did not differ between load 4 and load 6 (no identified clusters). However, the aperiodic-corrected alpha suppression was no longer associated with participants' working memory capacity (no identified clusters). Taken together, these findings indicate that the task- and load-dependent effects of alpha suppression represent true reductions in alpha-band oscillatory power as opposed to changes in aperiodic activity (fig. 10).

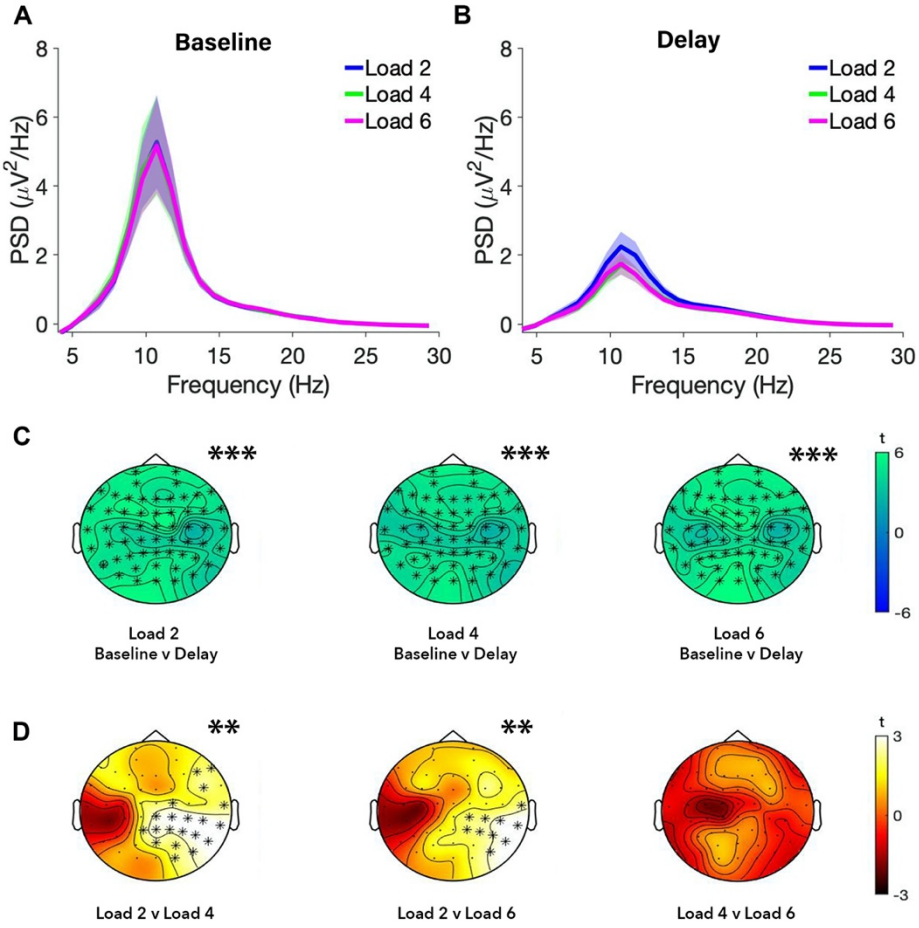

Figure 10. Aperiodic-corrected changes in alpha-band oscillatory power with working memory. A-B) EEG power spectra (power spectral density, PSD) during the baseline (A) and delay (B) period for each load following subtraction of aperiodic activity (the 1/f-like background of the PSD). Solid line represents the group mean and shaded bars the standard error. C) Topoplots indicating changes (t-statistics) in corrected alpha-band oscillatory power between the baseline and delay periods across all electrodes. D) Topoplots indicating differences in task-related alpha suppression between loads across all electrodes. * indicate electrodes contributing to significant clusters.

Relationship between EEG measures and working memory capacity

Finally, we asked whether the different EEG measures explained independent variance in working memory capacity. To examine the independent variance in working memory capacity explained by each EEG measure, we entered either the average of all electrodes contributing to a significant cluster when correlating the set size effect with working memory capacity or the electrode showing the peak correlation with working memory capacity as variables into a multiple linear regression model. Using the average of electrodes in a cluster explained 13.1% of variance (p = 0.004) in working memory capacity, with all variables providing independent contributions to the relationship, whereas using the peak correlation electrode explained 27.0% of variance ($p = 1.25 \times 10^{-5}$) with the aperiodic exponent and slow-wave ERP explaining independent variation (table 1). Together, these findings suggest that changes in the aperiodic exponent, slow-wave ERPs and alpha suppression index neural mechanisms that make distinct contributions to individual differences in working memory capacity.

Table 1. Parameter estimates from the multiple linear regression model for working memory capacity as a function of EEG measures.

	Average cluster		*Peak correlation*	
Variables	β	p	β	p
Aperiodic exponent	1.22	0.05	1.94	4.7×10^{-4}
Slow wave ERP	- 0.26	0.04	- 0.24	0.01
Alpha suppression	- 0.01	0.03	- 0.01	0.12

Discussion

The aim of this study was to comprehensively assess changes in broadband aperiodic activity in the EEG power spectrum during a visual working memory task. We found that characteristics of aperiodic activity were altered during the delay period of the task compared to a baseline period, with the aperiodic exponent increasing at fronto-central electrodes (i.e., slope of the power spectrum steepening), and decreasing (i.e., slope flattening) at lateral parieto-occipital electrodes. The broadband offset of the power spectrum also decreased across parieto-occipital electrodes during the delay period. Importantly, the task-related changes in aperiodic activity were not altered by different working memory loads. Across individuals, a larger task-related increase in the aperiodic exponent (i.e., steeper slope) over fronto-central electrode during supra-capacity loads (4 or 6 items) was associated with higher working memory capacity, a relationship which extended to performance on complex span working memory tasks collected separately from the EEG task. Finally, the relationship between task-related changes in the aperiodic exponent and working memory capacity was independent of other EEG correlates of capacity, including suppression of alpha-band oscillatory activity and slow-wave ERPs. Together, these findings suggest that task-related changes in the aperiodic exponent reflect a dissociable neural mechanism important for working memory ability.

The broadband 1/f-like power distribution is a well-recognized characteristic in neural recordings and is observed across numerous frequency ranges and different data types, including local field potentials, intracranial and scalp EEG, magnetoencephalography, and functional MRI (He, 2014). However, the physiological relevance of this broadband aperiodic activity is often overlooked with most analysis methods measuring narrow-band frequency ranges which potentially conflate rhythmic periodic activity with aperiodic activity (Donoghue et al., 2020). Studies which separate broadband aperiodic activity from periodic activity have demonstrated that aperiodic features of neural recordings are altered across a range of short and long timescales including with sensory stimuli and motor responses (Miller et al., 2014; Podvalny et al., 2015), from rest to task engagement (Donoghue et al., 2020), from wake to sleep (Lendner et al., 2020), and across the human lifespan (Schaworonkow & Voytek, 2021; Voytek et al., 2015). For example, Podvalny and colleagues (2015) found a reduction in the aperiodic exponent (i.e., flattening of

the power spectrum slope) in intracranial EEG recordings taken from task-related brain regions following visual, auditory, and motor events. Donoghue and colleagues (2020) found a reduction in both the aperiodic exponent and offset in scalp EEG recordings over lateral parieto-occipital regions during the delay period of a visual working memory task. In line with these findings, we also found a reduction in both the aperiodic exponent and offset at lateral parieto-occipital electrodes during a similar visual working memory task. However, we have expanded upon these findings by demonstrating that changes in the aperiodic exponent exhibit a different pattern across the scalp, increasing at fronto-central electrodes. Interestingly, the task-related changes in aperiodic exponent and offset were not modulated across different working memory loads, suggesting the differences in aperiodic activity may reflect a general change in task-related brain state which is independent of the number of items held in memory. Together, our findings support a growing body of evidence that aperiodic activity in the EEG power spectrum is modulated by cognitive tasks, the direction of which differs across the scalp.

Task-related changes in the slope of the power spectrum seem to reflect a physiological mechanism important for working memory. Several studies have reported a relationship between the aperiodic exponent and working memory performance, including from both scalp and intracranial EEG recordings (Donoghue et al.,2020; Gao et al., 2020; Voytek et al., 2015). Importantly, Donoghue and colleagues (2020) showed that a model including task-related changes in aperiodic exponent and offset values was better able to explain working memory performance compared to models including other neural correlates of working memory such as changes in alpha-band oscillatory power. We partially replicated and extended this finding, showing that larger task-related increases in aperiodic exponent values were related with higher working memory capacity independent of both alpha power suppression and changes in slow-wave ERP amplitude.

Alpha power suppression and lateralized slow-wave ERPs (known as contralateral delay activity) were once thought to measure a common neural mechanism (van Dijk et al., 2010). However, the measures are not related to one another in non-lateralised tasks, exist over a different time course, and explain independent variance in working memory capacity across individuals (Fukuda et al., 2015). In addition, studies using multivariate pattern analysis have shown that both stimulus position and feature information can be decoded from slow-wave ERPs, but only stimulus position from alpha-band oscillatory power (Bae

& Luck, 2017; Foster et al., 2017), suggesting the measures reflect different neural mechanisms relating to different aspects of working memory. Beyond task-specific performance, lateralised slow-wave ERPs during the delay period are related to measures of fluid intelligence, long-term memory, and attention control (Unsworth et al., 2015), suggesting this mechanism is important for broader cognitive ability. We have shown that the relationship between increases in the aperiodic exponent and capacity also extends beyond the task used in the EEG experiment, relating to measures of working memory performance obtained from complex span tasks. Complex span and non-selective visual array tasks like the continuous recall task in the current EEG experiment (e.g., not containing any distractor stimuli) share common variance which is thought to primarily reflect working memory storage capacity, with a small contribution from attention control (Draheim et al., 2020; Martin et al., 2019; Shipstead et al., 2015). Thus, our findings suggest that changes in the aperiodic exponent reflect a neural mechanism distinct from alpha power suppression and slow-wave ERPs which may be important for determining storage capacity limits in working memory. Future work measuring a broad range of cognitive tasks is required to further clarify the relationship between changes in the aperiodic exponent and other aspects of cognition relevant for working memory like attention control.

What are the neural mechanisms that could contribute to changes in aperiodic activity measured in the EEG power spectrum during visual working memory? Gao et al. (2017) used a biophysical model of excitatory and inhibitory neural populations and physiological data to demonstrate that the slope of the power spectrum measured by the aperiodic exponent in invasive recordings is sensitive to changes in the balance of excitatory and inhibitory neurotransmission, with a flattening slope indicating a greater excitation/inhibition balance and vice versa. In non-invasive recordings including EEG and MEG, anaesthetics and other pharmacological agents targeting excitatory and inhibitory receptors also alter the aperiodic exponent (Colombo et al., 2019; Muthukumaraswamy & Liley, 2018), suggesting excitation/inhibition balance is also reflected in scalp signals. Thus, the changes in the aperiodic exponent observed in our study could reflect a shift towards excitation over parieto-occipital regions and inhibition over frontal brain regions. Indeed, several recent studies using optogenetics (Kim et al., 2016), and recurrent neural networks (Kim & Sejnowski, 2021) have suggested that increased inhibitory-inhibitory

neurotransmission in frontal regions could underlie a lengthening of neural timescales which stabilises working memory performance. In contrast, changes in the broadband offset of the power spectrum in invasive recordings have been linked with changes in neuronal firing rates (Manning et al., 2009), with increased firing rates associated with increased offsets and vice versa. Thus, the reduction in the broadband offset over posterior regions may reflect a reduction in neuronal firing rates in parieto-occipital regions during the working memory delay period. Invasive recordings from visual (Van Kerkoerle et al., 2017) and parietal (Pesaran et al., 2002) regions in non-human primates typically suggest that neuronal firing rates either increase in task-relevant neurons, or return to baseline levels during the delay period, inconsistent with the above interpretation of our findings. The relationship between local-field potentials and scalp EEG can be complex (Snyder et al., 2018) and simultaneous invasive and non-invasive recordings are required to further clarify how changes in neural firing rates impact EEG power spectra measured at the scalp.

Our study is not without limitations. First, the EEG power spectra is contaminated by scalp muscle activity, which could impact measures of aperiodic activity including the aperiodic exponent and offset. We attempted to minimise this contamination by using a validated method to select and remove independent components likely representing muscle activity (Fitzgibbon et al., 2016), and by limiting our quantification of the power spectrum to lower frequencies (<30 Hz) which are thought to be less effected by muscle activity. However, these approaches are not foolproof, and also limit our capacity to detect changes in the higher-frequency ranges of the power spectrum, which likely carry important information on neural changes during working memory. Second, it is unclear from our study whether the changes in aperiodic activity are specific to working memory processes or reflect general changes in brain activity related to sensory processing or attention. Indeed, the lack of modulation of aperiodic activity with increasing memory load may indicate that these changes are not specific to working memory. Nonetheless, changes in the aperiodic exponent were related to performance across tasks, suggesting an important role for this neural mechanism in general working memory ability regardless of the specific sensory or cognitive process it underlies.

Overall, we provide evidence for region-specific changes in aperiodic activity during the delay period of a visual working memory task. Task-related changes in the slope of the power spectrum measured by the aperiodic exponent likely reflect a neural mechanism distinct from oscillatory and ERP changes also

observed during the task and appear important for general working memory ability. Our findings add to a growing body of evidence demonstrating the physiological relevance of aperiodic activity in brain function and underscore the importance of separating periodic and aperiodic activity when quantifying changes in EEG power spectra during cognitive tasks.

References

Baddeley, A. (2012). Working memory: Theories, models, and controversies. *Annual Review of Psychology, 63*, 1 - 29. https://doi.org/10.1146/annurev-psych-120710-100422

Bae, G.Y., & Luck, S. (2018). Dissociable decoding of spatial attention and working memory from EEG oscillations and sustained potentials. *Journal of Neuroscience, 38*(2), 409-422. https://doi.org/10.1523/JNEUROSCI.2860-17.2017

Berryman, C., Stanton, T.R., Bowering, K.J., Tabor, A., McFarlane, A., & Lorimer Moseley, G. (2013). Evidence for working memory deficits in chronic pain: A systematic review and meta-analysis. *Pain, 154*(8), 1181-1196. https://doi.org/10.1016/j.pain.2013.03.002

Chehreh-Negar, N., Shams, F., Zarshenas, S., & Nikseresht, A. (2012). Correlation between working memory and quality of life in multiple sclerosis patients. *KAUMS Journal (FEYZ)*, *16*(4), 337-345. https://doi.org/10.1186/1471-2377-11-17

Colombo, M. A., Napolitani, M., Boly, M., Gosseries, O., Casarotto, S., Rosanova, M., Brichant, J., Boveroux, P., Rex, S., Laureys, S., Massimini, M., Chieregato, A., & Sarasso, S. (2019). The spectral exponent of the resting EEG indexes the presence of consciousness during unresponsiveness induced by propofol, xenon, and ketamine. *Neuroimage*, *189*, 631-644. https://doi.org/10.1016/j.neuroimage.2019.01.024

Delorme, A., & Makeig, S. (2004). EEGLAB: an open source toolbox for analysis of single-trial EEG dynamics including independent component analysis. *Journal of Neuroscience Methods, 134*(1), 9-21. https://doi.org/10.1016/j.jneumeth.2003.10.009

Ding, W., Ding, L-J., Li, F-F., Han, Y., & Mu, L. (2015). Neurodegeneration and cognition in Parkinson's disease: a review. *European Review for Medical and Pharmacological Sciences, 19*(12)*,* 2275-2281. PMID: 26166654

DiStefano, C., & Motl, R. W. (2009). Self-esteem and method effects associated with negatively worded items: Investigating factorial invariance by sex. *Structural Equation Modeling*, *16*(1), 134-146. https://doi.org/10.1080/10705510802565403

Donoghue, T., Haller, M., Peterson, E.J., Varma, P., Sebastian, P., Gao, R., Noto, T., Lara, A.H., Wallis, J.D., Knight, R.T., Shestyuk, A., & Voytek, B. (2020). Parameterizing neural power spectra in periodic and aperiodic component. *Nature Neuroscience, 23,* 1655-1665. https://doi.org/10.1038/s41593-020-00744-x

Draheim, C., Tsukahara, J. S., Martin, J. D., Mashburn, C. A., & Engle, R. W. (2020). A toolbox approach to improving the measurement of attention control. *Journal of Experimental Psychology: General*, *150*(2), 242-275, https://doi.10.1037/xge0000783

Fitzgibbon, S. P., DeLosAngeles, D., Lewis, T. W., Powers, D. M. W., Grummett, T. S., Whitham, E. M., Ward, E.M., Willoughby, J.O., & Pope, K. J. (2016). Automatic determination of EMG-contaminated components and validation of independent component analysis using EEG during pharmacologic paralysis. *Clinical Neurophysiology*, *127*(3), 1781-1793. http://dx.doi.org/10.1016/j.clinph.2015.12.009

Foster, J.J., Sutterer, D.W., Serences, J.T., Vogel, E.K., & Awh, E. (2017). Alpha-band activity reveals spontaneous representations of spatial position in visual working memory. *Current Biology, 27*(20), 3216-3223. https://doi.org/10.1016/j.cub.2017.09.031

Foster, J.J., Sutterer, D.W., Serences, J.T., Vogel, E.K., & Awh, E. (2016). The topography of alpha-band activity tracks the content of spatial working memory. *Journal of Neurophysiology, 115,* 168-177. https://doi.org/10.1152/jn.00860.2015

Fukuda, K., Vogel, E., Mayr, U., Awh, E. (2010). Quantity, not quality: the relationship between fluid intelligence and working memory capacity. *Psychonomic Bulletin & Review, 17*(5), 673-679. https://doi.org/10.3758/17.5.673.

Fukuda, K., Mance, I., & Vogel, E.K. (2015). Alpha power modulation and event-related slow wave provide dissociable correlates of visual working memory. *The Journal of Neuroscience, 35*(41), 14009-14016. https://doi.org/10.1523/jneurosci.5003-14.2015

Gao, R., Peterson, E.J., & Voytek, B. (2017). Inferring synaptic excitation/inhibition balance from field potentials. *Neuroimage, 151,* 70-78. https://doi.org/10.1016/j.neuroimage.2017.06.078

Gao, R., van den Brink, R.L., Pfeffer, T., & Voytek, B. (2020). Neuronal timescales are functionally dynamic and shaped by cortical microarchitecture. *Elife*, 9:e61277. https://doi.org/10.7554/eLife.61277

Gevins, A., Smith, M. E., McEvoy, L., & Yu, D. (1997). High-resolution EEG mapping of cortical activation related to working memory: effects of task difficulty, type of processing, and practice. *Cerebral Cortex*, *7*(4), 374-385. https://doi.org/10.1093/cercor/7.4.374

Grice, J. W. (2001). Computing and evaluating factor scores. *Psychological Methods, 6*(4), 430-450. https://doi.org/10.1037/1082-989X.6.4.430

He, B. J. (2014). Scale-free brain activity: past, present, and future. *Trends in Cognitive Sciences 18*(9)*,* 480–487. https://doi.org/10.1016/j.tics.2014.04.003

Hyvärinen, A. (1999). Fast and Robust Fixed-Point Algorithms for Independent Component Analysis. *IEEE Transactions on Neural Networks 10*(3), 626-634. https://doi.org/10.1109/72.761722

Inquisit 5 [Computer software]. (2016). Retrieved from https://www.millisecond.com.

Jensen, O., & Mazaheri, A. (2010). Shaping functional architecture by oscillatory alpha activity: gating by inhibition. *Frontiers in Human Neuroscience, 4*,186. https://doi.org/10.3389/fnhum.2010.00186

Jokisch, D., & Jensen, O. (2007). Modulation of gamma and alpha activity during a working memory task engaging the dorsal or ventral stream. *The Journal of Neuroscience, 27*(12)*,* 3244–3251. https://doi.org/10.1523/JNEUROSCI.5399-06.2007

Kane, M. J., Hambrick, D. Z., Tuholski, S. W., Wilhelm, O., Payne, T. W., & Engle, R. W. (2004). The generality of working memory capacity: A latent variable approach to verbal and visuospatial memory span and reasoning. *Journal of Experimental Psychology: General, 133*(2), 189-217. https://doi.org/10.1037/0096-3445.133.2.189

Kim, D., Jeong, H., Lee, J., Ghim, J. W., Her, E. S., Lee, S. H., & Jung, M. W. (2016). Distinct roles of parvalbumin-and somatostatin-expressing interneurons in working memory. *Neuron*, *92*(4), 902-915. https://doi.org/10.1016/j.neuron.2016.09.023

Kim, R., & Sejnowski, T. J. (2021). Strong inhibitory signaling underlies stable temporal dynamics and working memory in spiking neural networks. *Nature Neuroscience*, *24*(1), 129-139. https://doi.org/10.1038/s41593-020-00753-w

Lendner, J. D., Helfrich, R. F., Mander, B. A., Romundstad, L., Lin, J. J., Walker, M. P., Larson, P.G., & Knight, R. T. (2020). An electrophysiological marker of arousal level in humans. *Elife*, *9*, e55092.

Logie, R.H. (2011). The functional organization and capacity limits of working memory. *Current Directions in Psychological Science, 20*(4), 240-245. https://doi.org/10.1177/0963721411415340

Luck, S. J., & Vogel, E. K. (2013). Visual working memory capacity: from psychophysics and neurobiology to individual differences. *Trends in Cognitive Sciences*, *17*(8), 391-400. https://doi.org/10.1016/j.tics.2013.06.006

Manning, J. R., Jacobs, J., Fried, I., & Kahana, M. J. (2009). Broadband shifts in local field potential power spectra are correlated with single-neuron spiking in humans. *Journal of Neuroscience*, *29*(43), 13613-13620. https://doi.org/10.1523/JNEUROSCI.2014-09-2009

Martin, J., Tsukahara, J. S., Draheim, C., Shipstead, Z., Mashburn, C., Vogel, E. K., & Engle, R. W. (2019). The visual arrays task: Visual storage capacity or attention control? *Journal of Experimental Psychology: General*, PMID: 34591545, https://doi.org/10.1037/xge0001048

McCollough, A. W., Machizawa, M. G., & Vogel, E. K. (2007). Electrophysiological measures of maintaining representations in visual working memory. *Cortex*, *43*(1), 77-94. http://doi.org/10.1016/S0010-9452(08)70447-7

Miller, K. J., Honey, C. J., Hermes, D., Rao, R. P., & Ojemann, J. G. (2014). Broadband changes in the cortical surface potential track activation of functionally diverse neuronal populations. *Neuroimage*, *85*, 711-720. https://doi.org/10.1016/jneuroimage.2013.08.070

Muthukumaraswamy, S. D., & Liley, D. T. (2018). 1/f electrophysiological spectra in resting and drug-induced states can be explained by the dynamics of multiple oscillatory relaxation processes. *NeuroImage*, *179*, 582-595. https://doi.org/10.1016/j.neuroimage.2018.06.068

Oostenveld, R., Fries, P., Maris, E., Schoffelen, J.M. (2011). FieldTrip: Open Source Software for Advanced Analysis of MEG, EEG, and Invasive Electrophysiological Data. *Computational Intelligence and Neuroscience,* (156869) https://doi.org/10.1155/2011/156869

Park, S., & Gooding, D. (2014). Working memory impairment as an endophenotypic marker of a schizophrenia diathesis. *Schizophrenia Research: Cognition, 1*(3), 127-136. https://doi.org/10.1016/j.scog.2014.09.005

Pesaran, B., Pezaris, J. S., Sahani, M., Mitra, P. P., & Andersen, R. A. (2002). Temporal structure in neuronal activity during working memory in macaque parietal cortex. *Nature Neuroscience*, *5*(8), 805-811. https://doi.org/10.1038/nn890

Podvalny, E., Noy, N., Harel, M., Bickel, S., Chechik, G., Schroeder, C.E., Mehta, A.D., Tsodyks, M., & Malach, R. (2015). A unifying principle underlying the extracellular field potential spectral responses in the human cortex. *Journal of Neurophysiology, 114*(1)*,* 505-519. https://doi.org/10.1152/jn.00943.2014

Rock, P.L., Roiser, J.P., Riedel, W.J., & Blackwell, A.D. (2014). Cognitive impairment in depression: a systematic review and meta-analysis. *Psychological Medicine, 44*(10)*,* 2029-2040. https://doi.org/10.1017/S0033291713002535

Rogasch, N.C., Sullivan, C., Thomson, R.H., Rose, N.S., Bailey, N.W., Fitzgerald, P.B., Farzan, F., Hernandez-Pavon, J.C. (2017). Analysing concurrent transcranial magnetic stimulation and electroencephalographic data: A review and introduction to the open-source TESA software. *Neuroimage, 15*(147), 934-951. https://doi.org/ 10.1016/j.neuroimage.2016.10.031.

Rossi, S., Hallett, M., Rossini, P.M., & Pascual-Leone, A. (2009). Safety, ethical considerations, and application guidelines for the use of transcranial magnetic stimulation in clinical practice and research. Clinical Neurophysiology, *120*(12), 2008-2039. https://doi.org/10.1016/j.clinph.2009.08.016.

Ruchkin, D. S., Johnson Jr, R., Grafman, J., Canoune, H., & Ritter, W. (1992). Distinctions and similarities among working memory processes: An event-related potential study. *Cognitive Brain Research*, *1*(1), 53-66. https://doi.org/10.1016/0926-6410(92)90005-c

Ruchkin, D. S., Canoune, H. L., Johnson Jr, R., & Ritter, W. (1995). Working memory and preparation elicit different patterns of slow wave event-related brain potentials. *Psychophysiology*, *32*(4), 399-410. https://doi.org/10.1111/j.1469-8986.1995.tb01223.x

Sawyer-Glover, A.M., & Shellock, F.G. (2000). Pre-MRI procedure screening: Recommendations and safety considerations for biomedical implants and devices. *Journal of Magnetic Resonance Imaging, 12*(1), 92-106. https://doi.org/10.1002/1522-2586(200007)12:1<92::AID-JMRI11>3.0.CO;2-7

Sauseng, P., Klimesch, W., Heise, K. F., Gruber, W. R., Holz, E., Karim, A. A., Glennon, M., Gerloff, C., Birbaumer, N., & Hummel, F. C. (2009). Brain oscillatory substrates of visual short-term memory capacity. *Current Biology*, *19*(21), 1846-1852. https://doi.org/10.1016/j.cub.2009.08.062

Schaworonkow, N., & Voytek, B. (2021). Longitudinal changes in aperiodic and periodic activity in electrophysiological recordings in the first seven months of life. *Developmental cognitive neuroscience*, *47*, 100895. https://doi.org/10.1016/j.dcn.2020.100895

Shipstead, Z., Harrison, T. L., & Engle, R. W. (2015). Working memory capacity and the scope and control of attention. *Attention, Perception, & Psychophysics*, *77*(6), 1863-1880. https://doi.org/10.3758/s13414-015-0899-0

Shipstead, Z., Redick, T. S., Hicks, K. L., & Engle, R. W. (2012). The scope and control of attention as separate aspects of working memory. *Memory*, *20*(6), 608-628. https://doi.org/10.1080/09658211.2012.691519

Snyder, A. C., Issar, D., & Smith, M. A. (2018). What does scalp electroencephalogram coherence tell us about long-range cortical networks? *European Journal of Neuroscience*, *48*(7), 2466-2481. https://doi.org.10.1111/ejn.13840

Suchow, J.W., Brady, T.F., Fougnie, D., & Alvarez, G.A. (2013). Modeling visual working memory with the MemToolbox. *Journal of Vision, 10*(9), 1-8. https://doi.org/10.1167/13.10.9

Tabachnick, B.G., & Fidell, L.S. (2019). *Using multivariate statistics* (7th ed.). Pearson.

Unsworth, N., Fukuda, K., Awh, E., & Vogel, E. K. (2015). Working memory delay activity predicts individual differences in cognitive abilities. *Journal of Cognitive Neuroscience*, *27*(5), 853-865.

https://doi.org/101162/jocn_a_00765

Unsworth, N., Heitz, R.P., Schrock, J.C., & Engle, R.W. (2005). An automated version of the operation span task. *Behavior Research Methods*, *37*, 498 - 505. https://doi.org/10.3758/BF0319720

van Dijk, H., van der Werf, J., Mazaheri, A., Medendorp, W.P., & Jensen, O. (2010). Modulations in oscillatory activity with amplitude asymmetry can produce cognitively relevant event-related responses. *PNAS, 107*(2), 900-905. https://www.pnas.org/content/107/2/900

Van Kerkoerle, T., Self, M. W., & Roelfsema, P. R. (2017). Layer-specificity in the effects of attention and working memory on activity in primary visual cortex. *Nature Communications*, *8*(1), 1-14. https://doi.org/10.1038/ncomms13804

Vogel, E. K., & Machizawa, M. G. (2004). Neural activity predicts individual differences in visual working memory capacity. *Nature*, *428*(6984), 748-751. https://doi.org/10.1038/nature02447

Vogel, E.K., McCollough, A.W., Machizawa, M.G. (2005). Neural measures reveal individual differences in controlling access to working memory. *Nature, 438*(24), 500-503. https://doi.org/10.1038/nature04171

Voytek, B., Kramer, M.A., Case, J., Lepage, K.Q., Tempesta, Z.R., Knight, R.T., & Gazzaley, A. (2015). Age related changes in 1/f neural electrophysiological noise. *The Journal of Neuroscience, 35*(38), 13257-13265. https://doi.org/10.1523/jneurosci.2332-14.2015

Woods, D.L., Kishiyamaa, M.M, Lund, E.W., Herron, T.J., Edwards, B., Poliva, O., Hink, R.F., & Reed, B. (2011). Improving digit span assessment of short-term verbal memory. *Journal of Clinical and Experimental Neuropsychology, 33*, 101-111. https://doi.org/10.1080/13803395.2010.493149